# Resonant coupling of oscillating gas or vapor bubbles in water: An experimental study

K. Ohsaka and E. H. Trinh

Jet Propulsion Laboratory, California Institute of Technology, Pasadena, California 91109

## ABSTRACT

A two-frequency acoustic apparatus is used to study resonant coupling of oscillating gas or vapor bubbles in water. First, the threshold amplitude of resonant coupling between the volume and axisymmetric shape oscillations is measured for gas bubbles in the shape modes, n = 3, 4, 5 and 6, and for vapor bubbles in the modes, n = 4 and 5, where n is the mode number. The results qualitatively agree with a theoretical prediction based on a phase-space analysis. Secondly, the efficiency of two coupling conditions, two-one (2:1) and one-one (1:1) resonant conditions is measured for the n = 4 and 5 modes. The results can be generalized as follows: When n is an even number, the (1:1) coupling condition has better energy transfer efficiency than (2:1). On the other hand, when n is an odd number, the (2:1) coupling condition has better energy transfer efficiency than (1:1).

mode coupling

## I. INTRODUCTION

Volume (radial) and/or shape oscillations of gas or vapor bubbles in fluids occur in natural phenomena and in industrial processes. Ambient noise in oceans is believed to be partially originated from oscillating gas bubbles created by rain, wind or breaking waves[1]. The efficiency of the distillation or heat transfer process is believed to be enhanced by cavitating vapor bubbles in fluids[2]. Thus, understanding of the fundamentals of the bubble dynamics is essential for better predictions of natural phenomena and more precise control of industrial processes.

Since bubble oscillations are intrinsically non-linear, resonant coupling between the volume and shape oscillations may play a significant role in some processes which are influenced by oscillating bubbles. For example, Longuest-Higgins showed that the monopole sound emission in oceans could be generated by the shape oscillations of bubbles[3,4]. Subsequent theoretical studies predicted unique features of the resonant interactions in terms of the energy transfer between the volume and shape modes[5-10]. Experimental evidence to corroborate some of the features has been reported[11]. In this paper, we present an experimental study which aims to determine the threshold amplitude of coupling and to compare the efficiency of coupling between the two-one and one-one coupling conditions.

## II. EXPERIMENTAL APPROACH

### A. Apparatus

We used an apparatus developed for the previous study[12]. The apparatus is capable of trapping a bubble by an ultrasonic standing wave while independently driving the bubble into oscillations using a second lower frequency acoustic wave. Since the implementation of the apparatus is previously described in detail[12], it is only briefly presented here. Figure 1 schematically shows the apparatus. The cell is a hollow cylindrical quartz tube and is

approximately half filled with water in which a bubble is trapped. The transducer is driven at around 104 kHz to create an ultrasonic standing wave for trapping a bubble. The broadband audio speaker generates sound pressure which is sufficient to drive the bubble into either volume or shape oscillation. The nichrome heaters wound around the cell are used to raise the water temperature. The oscillating bubble is back illuminated by a strobe light and its volume variation is captured by a standard camera with a telescopic lens. In addition, in this study, a high speed digital camera is used to sequentially capture the images of the shape oscillations in slow motion.

## B. Experimental procedure

### B.1. Threshold amplitude

Resonant coupling occurs between the volume and shape oscillations when the volume amplitude exceeds a threshold. The minimum amplitude of the volume oscillation required for inducing the shape oscillation was determined for the axisymmetric shape modes with low mode numbers. For this study, gas or vapor bubbles were initially driven in the volume oscillation at a frequency approximately twice of the resonant frequency of a shape mode. Then, the driving acoustic pressure was gradually increased until the shape oscillation was induced. Since the amplitude was linearly proportional to the driving acoustic pressure, the threshold amplitude could be calculated from the driving acoustic pressure at the onset of the shape oscillation by multiplying a linear coefficient. The linear coefficient was separately determined by measuring the amplitude at a reference driving sound pressure level. The procedure was repeated at different driving frequencies to determine the variation of the threshold amplitude around the resonant frequency. This measurement was performed for both gas and vapor bubbles.

### B.2. Effect of a surfactant on the threshold amplitude

When the bubble surface is covered with a surfactant, it shows surface elasticity and affects the damping of capillary waves. The effect of a surfactant on the threshold amplitude was studied by adding a small amount (approximately 0.1 % by volume) of 4-Decanone in the water. The measurement procedure was the same as the above. This measurement was performed for gas bubbles at room temperature.

### B.3. Efficiency of coupling

It is known that resonant coupling occurs when the ratio between the driving frequency and the resonant frequency of a shape oscillation is a small integer such as 1, 2 or 3, or a small number fraction such as 1/3, 1/2 or 2/3. We denote these coupling conditions as $(m_1:m_2)$, where $m_1$ and $m_2$ are integers and $m_1/m_2$ is given by the driving frequency divided by the resonant frequency. It is expected that the efficiency of the energy transfer from the volume to the shape oscillations varied depending on the coupling condition. For this study, we drove bubbles into a same shape mode with several different coupling conditions, specifically, (2:1), (1:1) and (2:3). There were no established ways to compare the efficiency of coupling, so we evaluated the efficiency using the following two methods:

Method A: Comparison of the amplitude of the shape and volume oscillations

First, we determined the amplitude of the volume oscillation at an acoustic pressure below the threshold value. Then, we gradually increased the pressure to induce the shape oscillation and determined the amplitude of the shape oscillation. The amplitude of the shape mode was calculated by dividing the variation of a representative linear dimension (explained later) of the shape by $2R_0$, where $R_0$ is the equilibrium radius of the bubble. For the comparison at the same acoustic pressure, the amplitude of the volume mode was linearly extrapolated to the pressure at which the amplitude of the shape mode was

determined. The amplitude ratio between the shape and volume modes provided a measure of the efficiency.

Method B: Decomposition of the amplitude into the shape and volume components

Observations made in the early stages of the study indicated that the coupled shape oscillations were not always pure shape oscillations even well above the threshold amplitude. They were rather a mixture of the shape and volume modes. This finding suggested that the amplitude could be divided into the volume and shape components. Then, the ratio of the two components could be used to measure the efficiency of coupling. First, we measured the variation of in linear dimension of the shape oscillation. Then, the variation was approximated by superposition of two sinusoidal curves, one curve represented the volume mode and the other represented the shape mode. The fraction given by the amplitude of the volume element divided by the total amplitude provided a measure of the efficiency.

The resonant frequency, $f_n$ of the shape oscillation with the mode, n, is calculated by

$$(2\pi f_n)^2 = (n-1)(n+1)(n+2)\frac{\sigma}{\rho a^3} \tag{1}$$

where $\sigma$ is the surface tension, a is the radius of the bubble and $\rho$ is the fluid density.

## C. Image analysis

The images of oscillating bubbles were taken either at 30 frames per second (f/s) under strobe illumination using a standard digital video camera or 1000 f/s under continuous illumination using a high speed digital camera. The standard camera was mainly used to capture the volume oscillation in slow motion to determine the radius of the bubble. The sequential images allowed us to measure the maximum and minimum radii from which we

determined the amplitude of the volume oscillation. The high speed camera was used to capture the shape oscillations. Since the resonant frequency of the shape oscillations in this study was around 1 kHz, the camera sequentially captured the images at the rate of one image per cycle. The phase angle of one image was slightly different from that of the previous image. As a result, when the frequency was higher than 1 kHz, the sequence of the images moved forward. On the other hand, when the frequency was lower than 1 kHz, the sequence of the images moved backward. The sequential images allowed us to measure the variation of a linear dimension of the shape.

## III. RESULTS

Figure 2 shows the result of the threshold amplitude measurement on gas bubbles at room temperature, approximately 25 °C. The bubbles were driven at the frequencies which satisfied the (2:1) resonant coupling condition. The relative amplitude is given by the amplitude divided by the equilibrium radius of the bubble. The data are connected to form the stability boundary of the volume oscillation. The legend in the figure (for example, 3-0.44) denotes the mode number of the induced shape oscillation followed by the equilibrium radius (mm) of the bubble. The following observations can be made from Fig. 2: a) The threshold amplitude increases as the driving frequency moves away from the resonant frequency. As a result, the boundary between the stable and unstable regions of the volume oscillation forms a wedge. b) The threshold amplitude is minimum but a finite value at the frequency which is twice of the resonant frequency. c) The angle of the wedge appears to increase as n increases. d) The minimum threshold amplitude appears to decrease as n increases.

Figure 3 shows the result of the threshold amplitude measurement on vapor bubbles at 80 °C. The bubbles were driven at the frequencies which satisfied the (2:1) resonant coupling conditions. The following observations can be made from Fig. 3: a) The

resonant frequency is lower than that of the gas bubble with the same radius due to the reduction in the surface tension. b) The wedge angle is smaller than that of the gas bubble in the same mode of the shape oscillation. c) The minimum threshold amplitude appears to be independent on the bubble radius.

Figure 4 shows the result of the threshold amplitude measurement on gas bubbles when the water contained 4-Decanone (0.1 % by volume). The mode of the shape oscillation is n = 5. For comparison, the threshold amplitude of pure water, taken from Fig. 2 is also shown in the figure. The effect of the surfactant is twofold. First, it lowers the resonant frequency by reducing the surface tension. The surface tension is reduced by approximately 20 %. Secondly, it raises the threshold amplitude by increasing the surface elasticity and viscosity.

Figure 5 shows the sequential images of gas bubbles oscillating in the axisymmetric shape modes, n = 3, 4 and 5. The magnifications of the images are the same for all images. The sequential images of each mode represent one cycle of the shape oscillation. The images were distorted in the horizontal direction because of the curvature of the cell wall in addition to the actual deformation due to the ultrasonic pressure for trapping. Since the actual deformation was minimal and the images were not optically distorted in the vertical direction, we measured the length of the vertical line which passed the center of the image to represent the motion of the shape oscillations. The average of a half length of the measured length is approximately equal to the equilibrium radius of the equivalent spherical bubble.

Figure 6 shows the result of the amplitude ratio determination. The amplitude ratio between the volume and n=4 shape oscillations was determined when the bubbles were driven with three different coupling conditions, (2:1), (1:1) and (2:3). The figure shows that the (1:1) coupling is more efficient than (2:1).

Figure 7 shows the variation of the linear length of the shape oscillation in the n=5 mode, where the linear length is a half of the length of the vertical line defined above. The linear length is analogous to the radius of spherical bubbles. The measured values are shown as the open circles. The coupling condition is (2:1) as indicated in the legend. The variation can be approximately represented by a sinusoidal curve for the shape oscillation. The variation shows two maxima per cycle, which can be understood by noting that the vertical length of the images 1 and 3 of the n = 5 oscillation in Figure 4 is identical. Since the amplitude cannot be decomposed into the volume and shape components, we assume that the volume component is zero, i.e., the efficiency of the energy transfer is 100 %. The observed resonant frequency is 1003 Hz, therefore, the figure shows one cycle of the shape oscillation. The resonant frequency is calculated to be 929 Hz using Eq. (1) with the surface tension taken to be 72 mN/m.

Figure 8 shows the variation of the n=5 shape oscillation driven with the (1:1) coupling condition. The measured values are approximated by the superposition of two sinusoidal curves shown at the top portion of the figure. These curves are shifted on the linear length axis for presentation, therefore, only the amplitude is valid. The ratio of the amplitude of shape oscillation over that of the volume oscillation is 1.5, therefore, the efficiency of the energy transfer is 60 %. The observed and the calculated resonant frequencies are 941 and 940 Hz, respectively.

Figure 9 shows the variation of the n=5 shape oscillation driven with the (2:3) coupling condition. The measured values are approximated by the superposition of two sinusoidal curves shown at the top portion of the figure. These curves are shifted on the linear length axis for presentation, therefore, only the amplitude is valid. The ratio of the amplitude of shape oscillation over that of the volume oscillation is 2.2, therefore, the efficiency of the energy transfer is 70 %. The observed and the calculated resonant frequencies are 990 and

994 Hz, respectively. The (2:1) coupling is more efficient than (1:1) for the n=5 shape oscillation judging from the results in Figs. 7, 8 and 9.

Figure 10 shows the variation of the n=3 shape oscillation driven with the (2:1) coupling condition. The observed and the calculated resonant frequencies are 1051 and 978 Hz, respectively. In this particular case, the n=2 shape oscillation is expected to be induced because it satisfies the (4:1) coupling condition with the volume oscillation and the (2:1) coupling condition with the n=3 shape oscillation. In fact, the variation contains a small fraction of the n=2 component shown at the top portion of the figure.

## IV. DISCUSSION AND SUMMARY

The results of the threshold amplitude measurement on gas bubbles are compared with the theoretical predictions by Feng and Leal[8]. The shape and the angle of the stability boundary qualitatively agree with the predictions. The threshold amplitude at the resonant frequency is minimum but a finite value which does not agree with the theory which predicts no threshold amplitude. This disagreement arises from the fact that the theoretical calculation does not include an appropriate damping (energy dissipation) of the oscillations. It is not known why the amplitude decreases as n increases in the present study. The amplitude should increase as n increases if damping plays a significant role to stabilize the volume oscillation[10]. It appears that the threshold amplitude of vapor bubbles is basically the same as that of gas bubbles except the frequency shift due to the reduction in the surface tension at elevated temperatures. It is not known why the wedge angle of vapor bubbles is smaller than that of gas bubbles in the present study. The increase in the threshold amplitude by addition of the surfactant can be explained by the enhanced damping caused by surfactant layers on the interface[13].

During the experiment, we noticed that on some occasions high frequency capillary waves were visible on the bubble surface even when the low frequency driving pressure

was not present. Although the ultrasound pressure was kept at a marginally sufficient level for trapping a bubble, it was still much higher than the driving pressure. The surface disturbances generally tend to induce shape oscillations, but it is not clear how the capillary waves interact with the volume oscillation in the present experiment. We experienced the difficulty to maintain vapor bubbles at constant radii because of the temperature fluctuation caused by convection of the water. The resonant condition was easily destroyed by drifting radius due to the temperature fluctuation. Both buoyancy force and acoustic streaming can generate convection. As a result, we could only measure the threshold amplitude for n = 4 and 5. The above unexplained results may be explained if we were able to account the effects of the ultrasonic standing wave and convection of water around the vapor bubbles.

Feng and Leal[8] predict that the energy transfer is generally periodic, which means that the ratio of the amplitudes of the volume and shape oscillations periodically changes as the mode of the oscillation swings from one extreme to the other. On the contrary, we observed that the mixed mode oscillation established a steady state, i.e., the ratio remained constant for at least tens of seconds. This fact allowed us to determine the amplitude ratio of the mixed mode oscillation at the steady state. Decomposition of the variation of the shape oscillations into sinusoidal curves is simple but should be considered as the first order approximation. It failed to closely approximate the variation when the mixed modes were complicated, such as (2:3) for n =5. However, it is still useful for the present purpose. Rigorously speaking, the shape should be described by the superposition of its normal modes which are expressed by the Legendre polynomial[14]. The distorted images of the bubbles prevented us to apply this method.

We compared the coupling efficiency of the resonant interactions at different coupling conditions for the axisymmetric shape oscillations, n=4 and 5. The comparison of the amplitude ratio indicates that the (1:1) coupling condition is more efficient than (2:1) for the n=4 mode. On the other hand, the decomposition of the amplitude into the volume and

shape components indicates that the (2:1) condition is more efficient than (1:1) for the n=5 mode. This difference can be understood by noting that the variation of the linear length of the n=4 mode has one maximum per cycle (see Fig. 5); therefore, the n=4 shape oscillation is efficiently excited when the driving frequency is the same as the resonant frequency. On the other hand, the n=5 mode has two maxima per cycle (see Fig. 5), therefore, the n=5 shape oscillation is efficiently excited when the driving frequency is twice of the resonant frequency. The present observation is different from a common perception of the (2:1) condition being better than (1:1). The present result should be true for any n (see n=3 in Figure 5), so it may be generalized as follows: When n is an even number, the (1:1) coupling condition has better energy transfer efficiency than (2:1). On the other hand, when n is an odd number, the (2:1) coupling condition has better energy transfer efficiency than (1:1). The coupling efficiency may affect the degree of the threshold amplitude of resonant coupling depending on the mode and the coupling condition, but we could not deduce the effect from the results in Figs. 2 and 3.

Finally, we presented Fig. 10 which could be evidence for the resonant coupling between the shape modes, n = 2 and 3. However, this particular case can be alternatively explained as coupling between the volume and n=2 shape modes. Therefore, further study is required to distinguish the difference between them.

## ACKNOWLEDGMENTS

The research described in the paper was carried out at the Jet Propulsion Laboratory, California Institute of Technology, under contract with the National Aeronautics and Space Administration.

## REFERENCES

[1] H. C. Pumphery, L. A. Crum and L. Bjorno, "Underwater sound produced by individual drop impacts and rainfall," J. Acoust. Soc. Am. **85**, 1518 (1989).

[2] K. -A. Park and A. E. Bergles, "Ultrasonic enhancement of saturated and subcooled pool boiling," Intl. J. Heat Mass Transfer **31**, 664 (1988).

[3] M. S. Longuet-Higgins, "Monopole emission of sound by asymmetric bubble oscillations. Part 1. Normal modes," J. Fluid Mech. **201**, 525 (1989).

[4] M. S. Longuet-Higgins, "Monopole emission of sound by asymmetric bubble oscillations. Part 2. An initial-value problem," J. Fluid Mech. **201**, 543 (1989).

[5] J. E. Ffowcs-Williams and Y. P. Guo, "On resonant nonlinear bubble oscillations," J. Fluid Mech. **224**, 507 (1991).

[6] M. S. Longuet-Higgins, "Resonant in nonlinear bubble oscillations," J. Fluid Mech. **224**, 531 (1991).

[7] S. M. Yang, Z. C. Feng and L. G. Leal, "Nonlinear effects in the dynamics of shape and volume oscillations for a gas bubble in an external flow," J. Fluid Mech. **247**, 417 (1993).

[8] Z. C. Feng and L. G. Leal, "On energy transfer in resonant bubble oscillations," Phys. Fluids **5A**, 826 (1993).

[9] Z. C. Feng and L. G. Leal, "Bifurcation and chaos in shape and volume oscillations of a periodically driven bubble with two-to-one internal resonance," J. Fluid Mech. **266**, 209 (1994).

[10] N. A. Gumerov, "Effect of acoustic radiation on the stability of spherical bubble oscillations," Phys. Fluids **10**, 1767 (1998).

[11] Y. Mao, L. A. Crum and R. A. Roy, "Nonlinear coupling between the surface and volume modes of an oscillating bubble," J. Acoust. Soc. Am. **98**, 2764 (1995).

[12] K. Ohsaka and E. H. Trinh, "Experimental study of bubble resonant oscillations using a two-frequency acoustic technique," submitted to J. Acoust. Soc. Am.

[13] T. J. Asaki, D. B. Thiessen and P. L. Marston, "Effect of an insolubable surfactant on capillary oscillations of bubbles in water: Observation of a maximum in the damping," Phys. Rev. Lett. **75**, 2686 (1995).

[14] E. H. Trinh, D. B. Thiessen and R. G. Holt, "Driven and freely decaying nonlinear shape oscillations of drops and bubbles immersed in a liquid: experimental results'" J. Fluid Mech. **364**, 252 (1998).

## CAPTIONS

Figure 1. Schematic diagram of experimental apparatus showing the key parts.

Figure 2. The threshold amplitude of resonant coupling between the volume and shape oscillations of the gas bubbles at 25 °C. The legend shows the mode number followed by the equilibrium radius (mm).

Figure 3. The threshold amplitude of resonant coupling between the volume and shape oscillations of the vapor bubbles at 80 °C. The legend shows the mode number followed by the equilibrium bubble radius (mm).

Figure 4. The threshold amplitude of the gas bubbles in the n = 5 mode when the water contains 0.1 % (by volume) of 4-Decanone. For comparison, the corresponding values for pure water is also shown.

Figure 5. The sequential images of oscillating gas bubbles in the n = 3, 4 and 5 modes. Each sequence represents one cycle of oscillations. The magnifications are the same for all images.

Figure 6. The amplitude ratio between the shape (n = 4) and the volume oscillations compared at the same driving acoustic pressure for three different coupling conditions, (2:1), (1:1) and (2:3).

Figure 7. The variation of a shape dimension of the bubble oscillating in the n = 5 mode with the (2:1) coupling condition. The open circles are the measured values. The continuous line is a sinusoidal curve to approximate the variation.

Figure 8. The variation of a shape dimension of the bubble oscillating in the n = 5 mode with the (1:1) coupling condition. The open circles are the measured values. The variation is decomposed into two sinusoidal curves, one is for the volume mode and other is for the shape mode, as shown at the top portion of the figure.

Figure 9. The variation of a shape dimension of the bubble oscillating in the n = 5 mode with the (2:3) coupling condition. The open circles are the measured values.

The variation is decomposed into two sinusoidal curves, one is for the volume mode and other is for the shape mode, as shown at the top portion of the figure.

Figure 10. The variation of a shape dimension of the bubble oscillating in the n = 3 mode with the (2:1) coupling condition. The open circles are the measured values. The variation is decomposed into two sinusoidal curves, one is for the n =3 mode and other is for the n = 2 mode, as shown at the top portion of the figure.

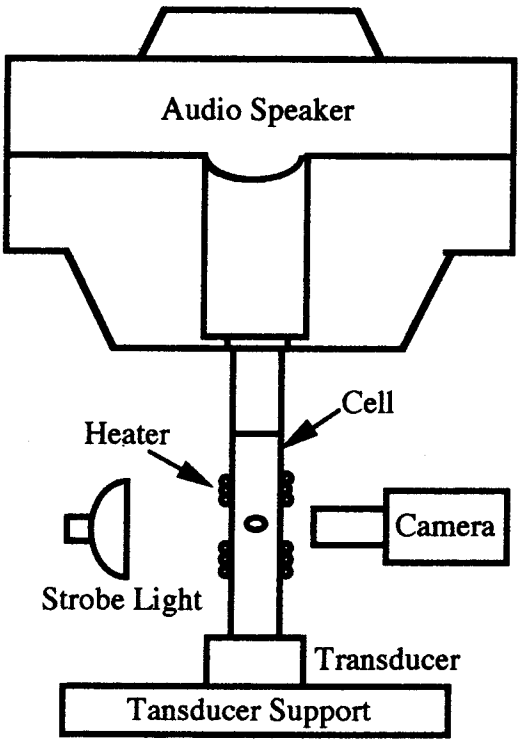


Fig. 1. K. Ohsaka, Phys. Fluids

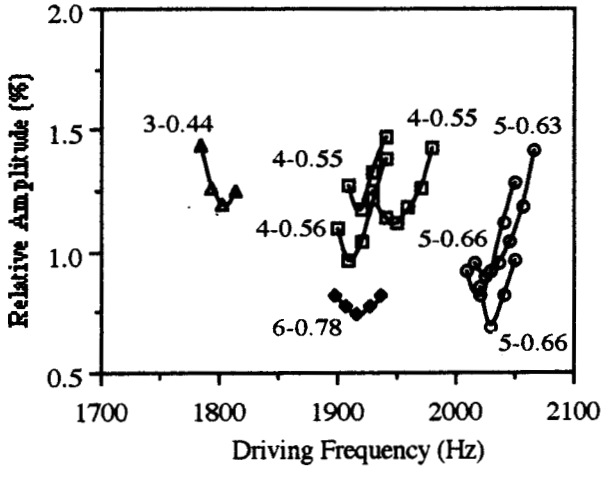


Fig. 2. K. Ohsaka, Phys. Fluids

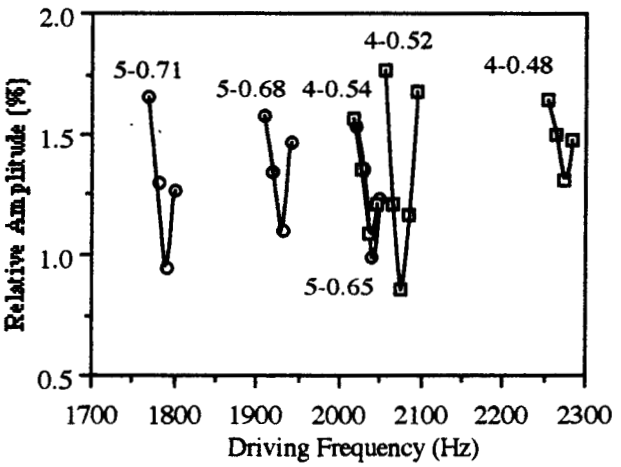


Fig. 3 K. Ohsaka Phys. Fluids

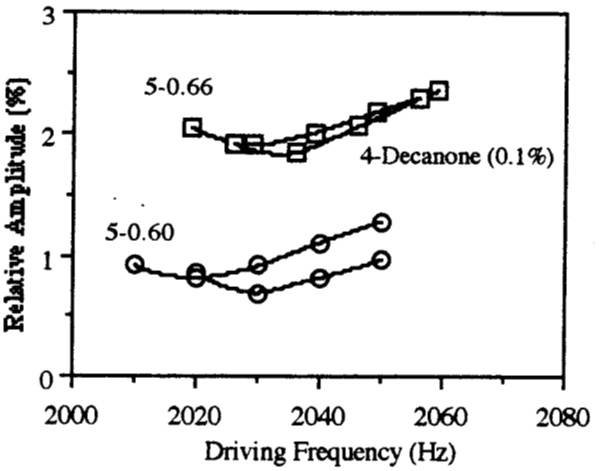


Fig. 4. K. Ohsaka Phys. Fluids

n = 3

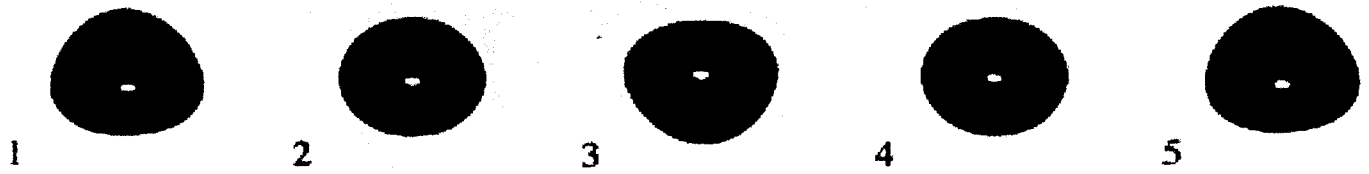


n = 4

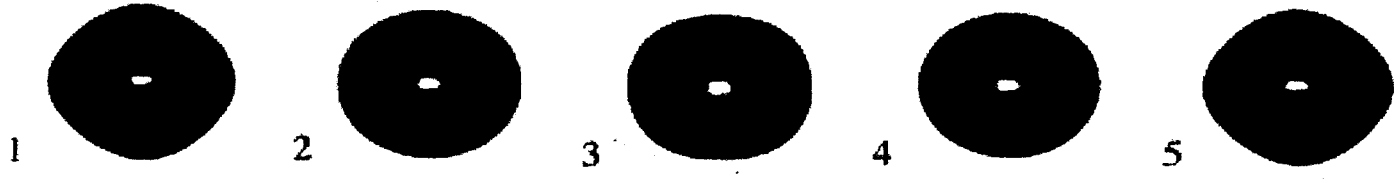


n = 5

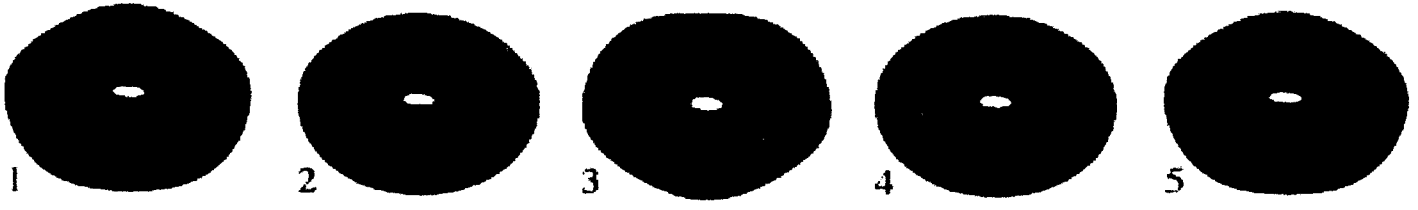


Fig 5 A Chladni Plate

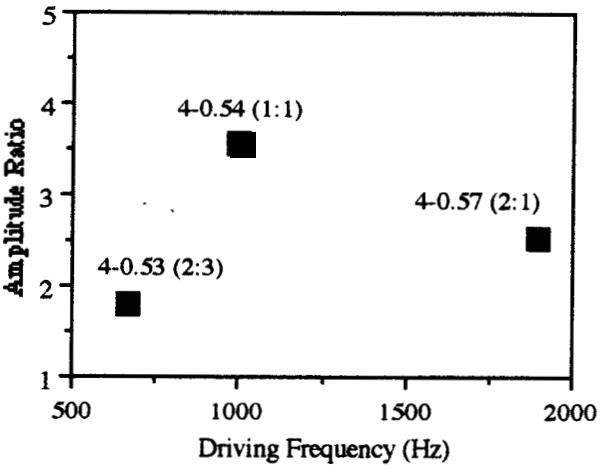


Fig. 6. K. Ohsaka, Phys. Fluids

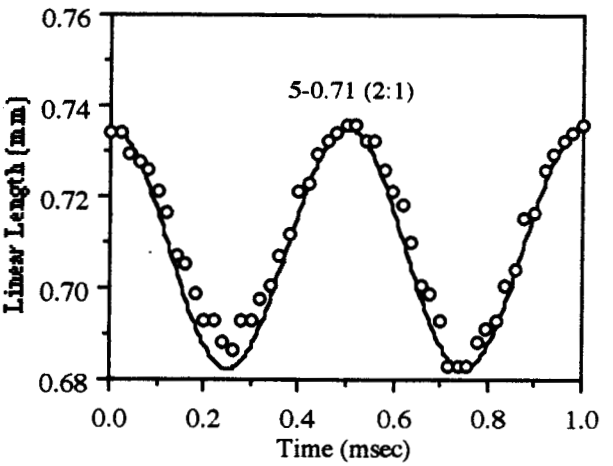


Fig. 7 K. Ohsaka Phys. Fluids

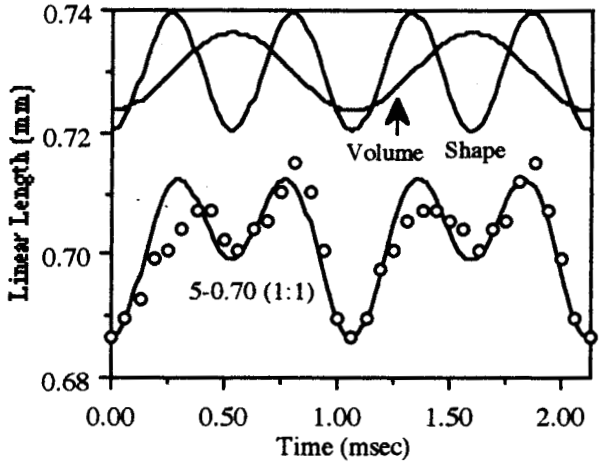


Fig. 8 K. Ohsaka Phys. Fluids

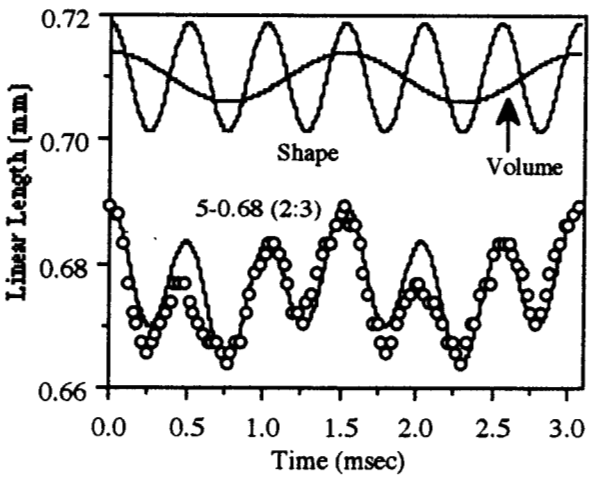


Fig 9. K. Ohsaka Phys. Fluids

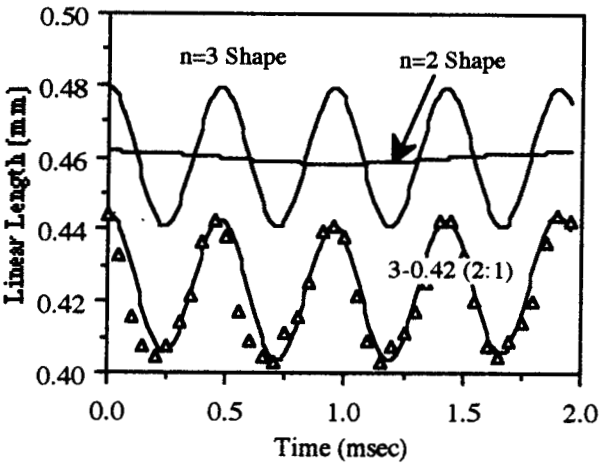


Fig. 10. K. Ohsaka Phys. Fluids